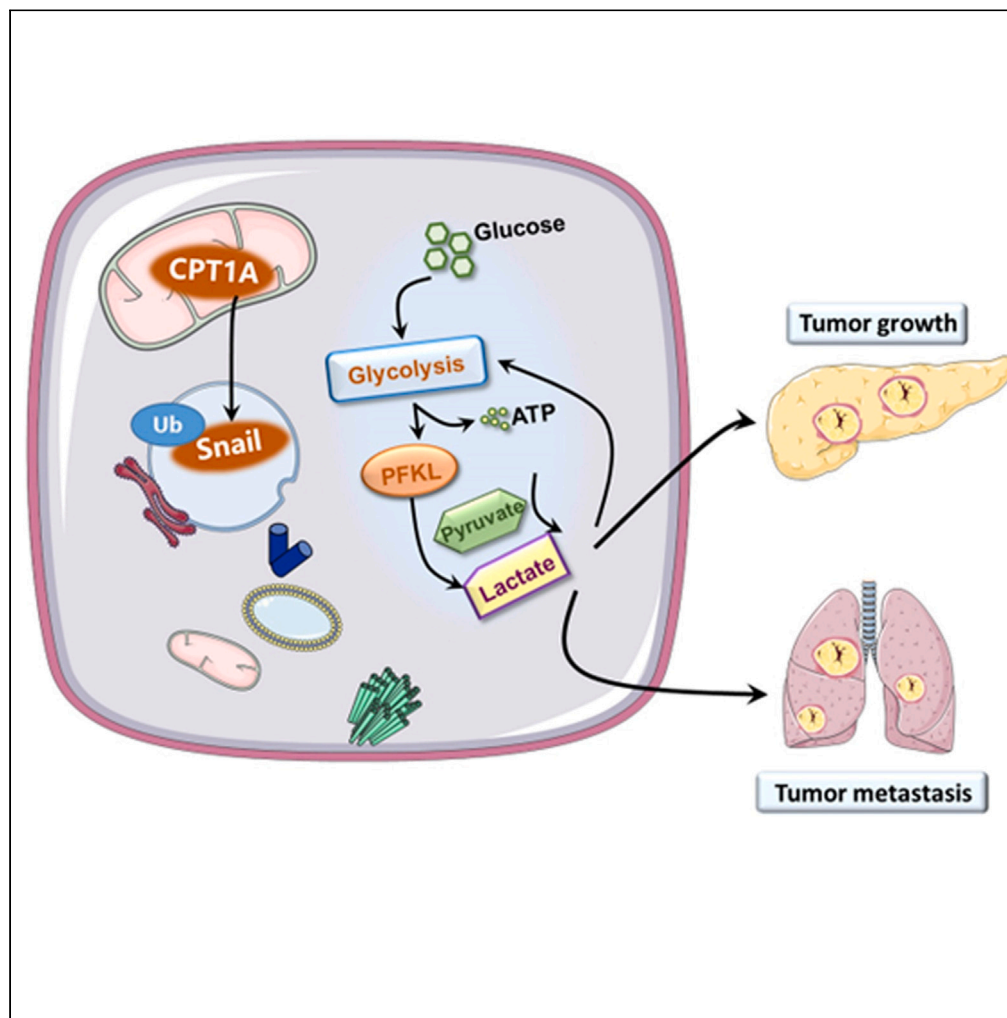


Article

The CPT1A/Snail axis promotes pancreatic adenocarcinoma progression and metastasis by activating the glycolytic pathway



Shipeng Yang,
Ying Liu, Chunxiao
Tang, Anna Han,
Zhenhua Lin, Jishu
Quan, Yang Yang

yangyang@ybu.edu.cn

Highlights

CPT1A upregulation
predicts poor prognosis of
PAAD

CPT1A promotes the
progression of PAAD by
activating the glycolytic
pathway

Targeting the CPT1A/
Snail/glycolysis in PAAD is
a potential treatment
strategy

Article

The CPT1A/Snail axis promotes pancreatic adenocarcinoma progression and metastasis by activating the glycolytic pathway

Shipeng Yang,^{1,2,3} Ying Liu,² Chunxiao Tang,² Anna Han,² Zhenhua Lin,^{1,2} Jishu Quan,² and Yang Yang^{1,2,3,4,*}

SUMMARY

Recent studies have demonstrated that CPT1A plays a critical role in tumor metabolism and progression. However, the molecular mechanisms by which CPT1A affects tumorigenicity during PAAD progression remain unclear. In the current research, the bioinformatics analysis and immunohistochemical staining results showed that CPT1A was overexpressed in PAAD tissues and that its overexpression was associated with a shorter survival time in patients with PAAD. Overexpression of CPT1A increased cell proliferation and promoted EMT and glycolytic metabolism in PAAD cells. Mechanistically, CPT1A is able to bind to Snail and facilitate PAAD progression by regulating Snail stability. In summary, our findings revealed Snail-dependent glycolysis as a crucial metabolic pathway by which CPT1A accelerates PAAD progression. Targeting the CPT1A/Snail/glycolysis axis in PAAD to suppress cell proliferation and metastatic dissemination is a new potential treatment strategy to improve the anticancer therapeutic effect and prolong patient survival.

INTRODUCTION

Pancreatic adenocarcinoma (PAAD) is the most fatal disease, with a 5-year survival rate of less than 9%, and it is expected to be the second leading cause of cancer-associated mortality worldwide by 2030.^{1,2} The metastatic tendency and resistance to traditional chemotherapy of PAAD are considered to result from the dearth of clinically targeted mutations, altered metabolism, tumor heterogeneity and the hypoxic microenvironment with immune cell exhaustion. Due to the dearth of archetypal clinical features and useful diagnostic methods, curative resection is not possible in most patients with PAAD.³ Despite this knowledge of the genetic characteristics of PAAD, therapeutic efforts to target the key carcinogenic factor Kirsten rat sarcoma (KRAS) have been largely unsuccessful thus far. Therefore, new treatment strategies are needed to specifically target cancer-specific pathways for the successful treatment of PAAD.

Metabolic reprogramming is one of the main events affecting tumor progression, metastasis, and prognosis and is characterized by activated glycolysis in multiple solid tumors, including PAAD.^{4,5} The preference of cancer cells for aerobic glycolysis is called the Warburg effect and is a classical metabolic reprogramming process in PAAD cells, supplying large amounts of ATP and lactate and producing the lowest amounts of reactive oxygen species (ROS) during the proliferation, DNA replication, and metastasis of PAAD cells.⁶ We recently discovered that promoting metabolism of saturated fat via fatty acid oxidation (FAO) by means such as supplying dietary palmitates, maintains mitochondrial homeostasis.⁷ It has also been indicated that tumor cells are able to reactivate oxidative phosphorylation (OXPHOS), in addition to activating the basic glycolytic pathway, to meet the increasing demand for cellular fuel and surviving genotoxic anticancer treatments.^{8,9} FAO is considered to play a committed role in mitochondrial lipolysis, enhancing tumor metabolism, and targeting key FAO enzymes increases the efficacy of cancer cell control.^{10–13}

As a rate-limiting enzyme in FAO, carnitine palmitoyl transferase system 1 (CPT1) is located in the outer mitochondrial membrane, transports free fatty acids (FFAs) into the mitochondrial matrix, where they are oxidized to acetylcarnitines.¹⁴ Ketone bodies generated via FAO function as a substitute energy source when the glucose supply is exhausted and accelerate cancer progression.¹⁵ The CPT1 family is composed of three isoforms, CPT1A, CPT1B, and CPT1C. Previous studies have confirmed that CPT1A is overexpressed in many cancers, including breast cancer, liver cancer, and glioma, and has become an undeveloped metabolic target in oncotherapy.^{16–18} Additionally, researchers have found that CPT1A expression is increased at colorectal carcinoma (CRC) metastatic tumor sites, and it drives the growth and extends the survival of detached CRC cells by mediating FAO pathway activity.¹⁹ Moreover, Tian et al.²⁰ confirmed that CPT1A expression leads to anoikis resistance in esophageal squamous cell carcinoma (ESCC) via redox homeostasis. However, the role of CPT1A in glycolytic metabolism in PAAD remains unclear.

¹Central Laboratory, The Affiliated Hospital of Yanbian University, Yanji 133000, China

²Key Laboratory of Tumor Pathobiology (Yanbian University), State Ethnic Affairs, Commission, Yanji 133000, China

³Department of Pathology, Yanbian University Medical College, Yanji 133000, China

⁴Lead contact

*Correspondence: yangyang@ybu.edu.cn

<https://doi.org/10.1016/j.isci.2023.107869>



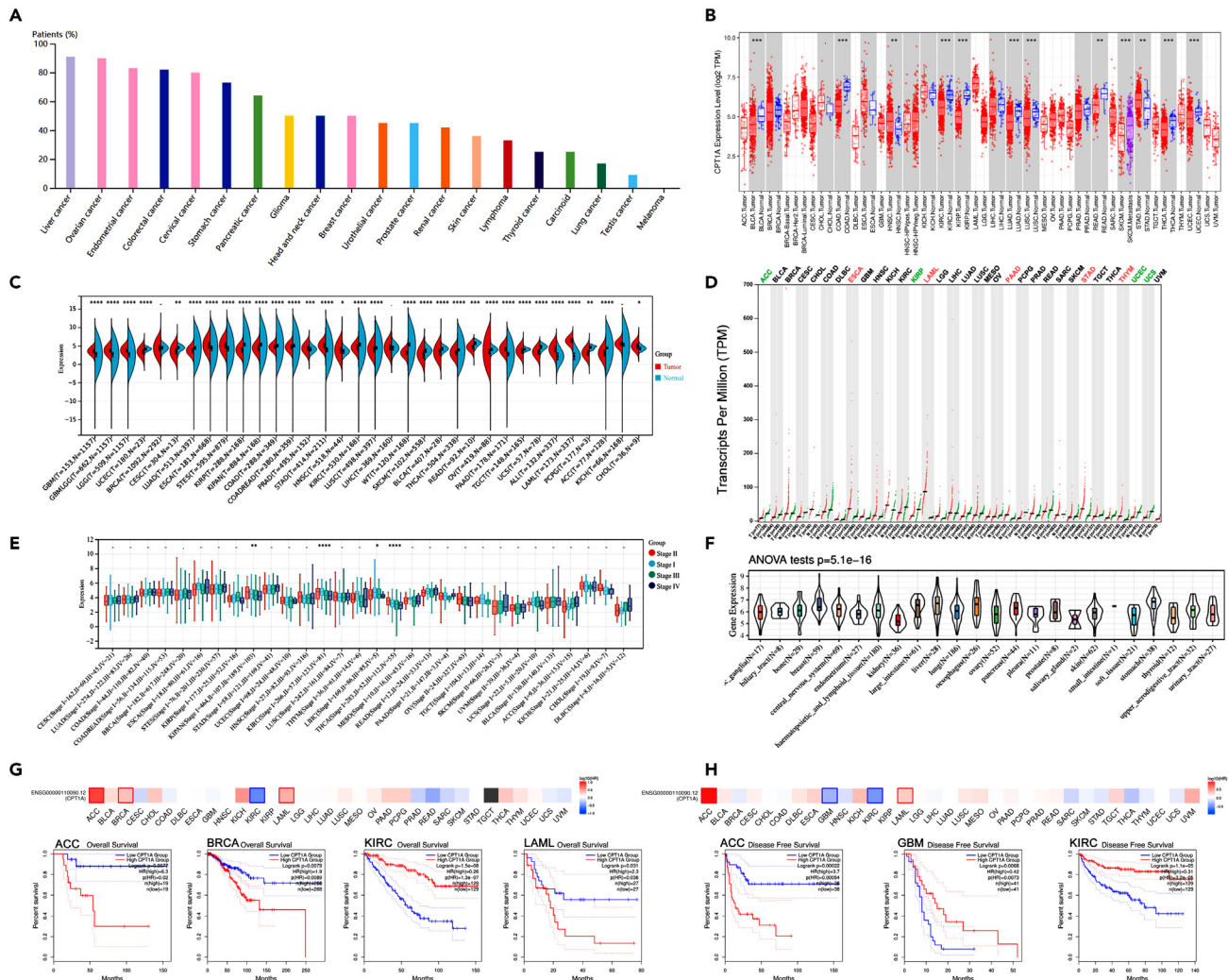


Figure 1. CPT1A is upregulation in pan-cancer and correlates with a poor outcome

(A) The mRNA expression of CPT1A in pan-cancers from the HPA database. (B–D) The mRNA expression of CPT1A in pan-cancers compared with normal tissues from TIMER (B), GEPIA (C), and UCSC (D) databases. (E) The relationship between the expression of CPT1A and the clinical stage of pan-cancer from the UCSC database. (F) The mRNA expression of CPT1A in different cancer cell lines from CCLL database ($p < 0.001$). (G and H) Kaplan-Meier survival analysis showed the OS (G) and DFS (H) of cancerous patients with CPT1A low or high expression in GEPIA database. * $p < 0.05$, ** $p < 0.01$, *** $p < 0.001$ and **** $p < 0.0001$.

Herein, we demonstrated that CPT1A could drive cell growth, cell metastasis, and Snail ubiquitination in PAAD through the glycolytic pathway, suggesting that the CPT1A/Snail axis might be an undeveloped treatment target for PAAD.

RESULTS

CPT1A was abnormally expressed across human cancers

Analysis of the HPA cohort revealed that the mRNA expression of CPT1A is high in most patient-derived cancer tissues, especially those from patients with gastrointestinal cancer and gynecological neoplasms (Figure 1A). Analysis of the TIMER database also indicated that the mRNA expression of CPT1A was higher in a variety of tumor subtypes, such as HNSC (head and neck squamous cell carcinoma) and STAD (stomach adenocarcinoma) (Figure 1B; all $p < 0.01$). The UCSC and GEPIA2 databases were used to further analyze the CPT1A level in the abovementioned cancers with obvious differential expression between tumors and normal tissues. We found that the mRNA expression of CPT1A was significantly higher in gastrointestinal cancer tissues than in normal tissues, especially in PAAD (Figures 1C and 1D; all $p < 0.05$). The trend in CPT1A mRNA expression from the early stage to the late stage of disease in patients with cancers was also summarized, and significant correlations were found, mainly in KIPAN (the pancreatic cohort), KIRC (kidney renal clear cell carcinoma), LIHC, and THCA (Figure 1E). Moreover,

Figure 2. Continued

- (E) Statistical results of IHC that CPT1A protein expression positive and strongly positive staining rates in adjacent non-tumor tissues and PAAD tissues.
- (F) Correction between CPT1A expression and clinicopathological significance of PAAD was shown in the Sankey diagram.
- (G) ROC curve analysis of the significant diagnostic value of CPT1A in patients with PAAD.
- (H) Kaplan-Meier survival analysis of patients with PAAD (n = 100) with CPT1A low or high expression (p = 0.001).
- (I and J) Forest plots showed the results of univariate (I) and multivariable (J) logistic regression analysis. *p < 0.05 and **p < 0.01.

the expression level of CPT1A was high in a panel of gastrointestinal cancer cell lines from the CCLE, as shown in Figure 1F (p = 5.1e-16). Kaplan-Meier survival analysis showed that patients with ACC (adrenocortical cancer) with high CPT1A expression had shorter OS and DFS times than those with low CPT1A expression. In addition, patients with KIRC with low CPT1A expression had significantly poorer outcomes (Figures 1G and 1H, all p < 0.05). Together, these data suggested that CPT1A was abnormally expressed across cancers and that its abnormal expression was closely related to malignant progression and prognosis in patients.

CPT1A upregulation predicts poor prognosis of pancreatic adenocarcinoma

Genetic alterations in CPT1A may cause its abnormal expression in cancers. According to data retrieved from the cBioPortal website, CPT1A has a high frequency of alterations, mainly amplification and mutation (Figure 2A). However, the alteration frequency was only 2.17% in PAAD; thus, we further explored the clinical value of CPT1A in PAAD. The mRNA expression of CPT1A was markedly increased in PAAD tissues from the TCGA and GEPIA databases (Figures 2B and 2C, both p < 0.05). Correspondingly, IHC staining showed that the CPT1A expression level was significantly increased in PAAD tissues compared with nontumor pancreatic tissues (Figure 2D). In this analysis, 22 of 80 nontumor pancreatic tissues (positive rate: 27.5%) and 84 of 100 PAAD tissues (positive rate: 84.0%) were found to be positive for CPT1A expression (p < 0.01); importantly, the rate of strong positive CPT1A expression in PAAD tissues (67/100, 67.0%) was higher than that in nontumor pancreatic tissues (10/80, 12.5%; p < 0.01) (Figure 2E, and Table 1). Furthermore, analysis of clinicopathological features showed that the expression level of CPT1A was positively correlated with sex (p = 0.219), LN metastasis status (p = 0.027), grade (p = 0.038) and diabetes history (p = 0.018), as shown in the forest plot (Figure 2F, and Table 2). The significant diagnostic value of CPT1A in patients with PAAD was assessed using ROC analysis (Figure 2G). These observations indicated that CPT1A might play a vital role during the occurrence and development of PAAD.

Subsequently, Kaplan-Meier analysis of patients revealed that OS was closely related to the expression of CPT1A (p = 0.000) and that a high level of CPT1A expression implied a poorer prognosis than did a low level (Figure 2H). In particular, compared with patients with low CPT1A expression, patients with high CPT1A expression and LN metastasis status (–) (p = 0.010), AJCC stage of IIB-IV (p = 0.009), low histological grade (p = 0.023), and history of diabetes (–) (p = 0.004) had significantly decreased OS times (Figure S1). The results of univariate logistic regression analysis showed that the overexpression of CPT1A was related to LN metastasis status, AJCC stage, histological grade and diabetes history in patients with PAAD (Figure 2I; and Table 3). Additionally, multivariate Cox regression analysis showed that CPT1A expression and histological grade could be independent prognostic markers in PAAD (Figure 2J). And diabetes history could be a correlated marker in PAAD. Hence, we concluded that CPT1A may prove to be an important prognostic index in PAAD.

CPT1A drives growth and inhibits autophagy in pancreatic adenocarcinoma cells

To further explore the functions of CPT1A in PAAD, BxPC-3 and PANC-1 cells were divided into four groups, namely Con, sh-CPT1A, Vector, and CPT1A overexpression groups, for lentiviral transduction. Assessment of the transduction efficiency by Western blotting showed that CPT1A expression was clearly suppressed in the sh-CPT1A #3 group compared to the Con group (Figures 3A and S2A). But, the transfection effects of CPT1A in BxPC-3 is better than in PANC-1. Subsequently, the proliferative capacity of cells was evaluated by an MTT assay, a colony formation assay, and an EdU incorporation assay. The results revealed that silencing CPT1A inhibited proliferation, colonization, and DNA replication in PAAD cells, while overexpression of CPT1A had the opposite effects (Figures 3B–3D). Under various conditions, autophagy can extend cell survival or increase cell death. We next sought to clarify the function of CPT1A in autophagy by AO staining in PAAD cells, as shown in Figure 3E. Compared with that in the corresponding control group, the number of autophagosomes (red) was increased in the sh-CPT1A group but reduced in the CPT1A-overexpressing group, indicating that silencing CPT1A elicited an autophagic response in PAAD cells. Consistent with this result, the protein expression levels of autophagy markers (Beclin-1 and LC3B) were increased in sh-CPT1A cells and decreased in CPT1A-overexpressing cells, as shown by Western blotting (Figures 3F and S2B). The results of *in vivo* experiments further confirmed the facilitation of neoplasm formation by CPT1A. Gross observation and evaluation of representative fluorescence images

Table 1. CPT1A protein expression in PAAD

Diagnosis	No. of cases	CPT1A protein expression				Positive rate	Strongly positive rate
		-	+	++	+++		
Normal	80	58	12	7	3	27.5%	12.5%
PAAD	100	16	17	35	32	84.0%**	67.0%**

*p < 0.05 and **p < 0.01: compared with non-tumor pancreas tissues.

PAAD: Pancreatic adenocarcinoma.

Table 2. Correlation between CPT1A expression and the clinicopathological features of PAAD

Variables	No. of cases	CPT1A strongly positive cases (%)	χ^2	p-value
Age (years)			1.126	0.289
<60	47	29 (61.70)		
≥60	53	38 (71.70)		
Gender			1.510	0.219
Male	63	45 (71.43)		
Female	37	22 (59.46)		
Tumor size (cm)			0.001	0.971
<4	79	53 (67.09)		
≥4	21	14 (66.67)		
LN metastasis			4.886	0.027
Negative	54	31 (57.41%)		
Positive	46	36 (78.26%)		
AJCC stage			1.166	0.280
I-IIA	56	35 (62.50)		
IIB-IV	44	32 (72.73)		
Histological grade			4.322	0.038
High/moderate	68	41 (60.29)		
Low	32	26 (81.25)		
Vessel infiltration			2.766	0.096
Negative	58	35 (60.34)		
Positive	42	32 (76.19)		
Diabetes history			5.593	0.018
No	56	32 (57.14)		
Yes	44	35 (79.55)		

indicated that the tumor size and weight were reduced in the sh-CPT1A group and increased in the CPT1A overexpression group (Figures 3G and S3A). However, there are some differences between BxPC-3 and PANC-1. The difference may be related to the natural inhibitor malonylCoA in two cell lines, and the role of malonylCoA in autophagy. Moreover, IHC staining of xenograft tumor sections also revealed that Ki67 expression was downregulated in the sh-CPT1A group and upregulated in the CPT1A overexpression group (Figures 3H, S3B, and S3C). These observations revealed that CPT1A plays a key oncogenic role in PAAD.

CPT1A accelerates pancreatic adenocarcinoma cell metastasis through EMT

According to the results of public database analysis, the CPT1A expression level was higher in SKCM (skin cutaneous melanoma) with metastasis than in SKCM (skin cutaneous melanoma) without metastasis (Figure 1B, $p < 0.01$). Hence, we became interested in investigating the biological functions of CPT1A in the dissemination of PAAD cells. As expected, downregulation of CPT1A significantly suppressed the lateral and longitudinal motility of PAAD cells compared with the Con cells, as proven in the wound healing, migration, and invasion assays, but enhanced the motility of CPT1A-overexpressing cells (Figures 4A, 4B, and S4A). Moreover, counting of lung nodules (Figure 4C) and H&E staining of lung tissues (Figure 4D) further confirmed that the downregulation of CPT1A markedly suppressed and upregulation of CPT1A promoted lung metastasis. More interestingly, the epithelial markers E-cadherin and ZO-1 were upregulated in CPT1A knockdown cells, while mesenchymal markers (ZEB-1, Vimentin, and Snail) were downregulated, and the opposite changes were found in CPT1A-overexpressing cells (Figures 4E and S2C). Consistent with the prediction results, the results of IF staining (Figure 4F) in PAAD cells and IHC staining in xenograft tumor sections (Figure 4G) further validated our observations that Vimentin expression was decreased in the sh-CPT1A groups but increased in the CPT1A-overexpressing groups. These observations demonstrated that CPT1A expression was closely associated with EMT progression in PAAD.

CPT1A promotes the malignant progression of pancreatic adenocarcinoma cells by activating the glycolytic pathway

In metastatic cancer cells, glycolytic metabolic reprogramming is indispensable for the colonization of distant organs, as distant sites have completely different nutritional energy sources and metabolic environments (Peng et al., 2021). Analysis of the GDS1883 and GDS1913

Table 3. Univariate and multivariate survival analyses (Cox regression model) of various factors in 100 patients with PAAD

Characteristics	B	SE	Wald	95% CI		p-value
				Lower	Upper	
Univariate survival analyses						
CPT1A	0.847	0.225	14.122	1.499	3.626	0.000
Age	0.163	0.202	0.647	0.791	1.750	0.421
Gender	0.100	0.214	0.218	0.727	1.679	0.138
Tumor size	−0.059	0.252	0.055	0.576	1.543	0.943
LN metastasis	0.609	0.211	8.334	1.216	2.782	0.004
AJCC stage	0.599	0.211	8.051	1.203	2.751	0.005
Histological grade	0.558	0.217	6.598	1.141	2.675	0.010
Vessel infiltration	0.176	0.206	0.731	0.797	1.784	0.392
Diabetes history	0.495	0.206	5.751	1.095	2.456	0.016
Multivariate survival analyses						
CPT1A	0.602	0.239	6.359	1.144	2.916	0.012
LN metastasis	0.251	0.511	0.241	0.472	3.502	0.623
AJCC stage	0.422	0.505	0.696	0.566	4.105	0.404
Histological grade	0.632	0.235	7.251	1.188	2.982	0.007
Diabetes history	0.586	0.221	6.996	1.164	2.772	0.008

B: Coefficient; SE: standard error; Wald: Wald statistic; CI: confidence interval.

datasets revealed that the expression of CPT1A was significantly upregulated in diabetic *Rattus norvegicus* compared with healthy *Rattus norvegicus* (Figure 5A), suggesting that the expression of CPT1A is closely related to glucose metabolism. Subsequently, glucose, lactate and ATP assay kits were used, and the results of these assays showed that the downregulation of CPT1A attenuated glucose levels, while CPT1A overexpression had the opposite effects (Figure 5B). Furthermore, we investigated the effects of CPT1A on glycolytic enzymes by Western blotting, and the results showed that the glycolytic enzymes HK, GLUT, PFKL, LDHA and PKM2 were downregulated in sh-CPT1A cells, and this downregulation was reversed by CPT1A overexpression (Figures 5C and S2D). The above results supported the conclusion that CPT1A promoted glycolytic pathway activity in PAAD cells. To further verify the oncogenic role of CPT1A in PAAD, the effects of a CPT1A inhibitor (etomoxir) were evaluated by MTT, colony formation, and transwell assays. The results revealed that treatment with etomoxir decreased the proliferation, and colonization, migration ability of PAAD cells compared with CPT1A-overexpressing cells (Figures S5A–S5C). Moreover, etomoxir treatment significantly weakened the effects of CPT1A on EMT and glycolytic pathway in PAAD cells (Figures S5D–S5E). The above results suggested that CPT1A plays an important role in promoting the progression of PAAD.

To further clarify the regulatory mechanism of the glycolytic pathway in PAAD, the effects of glycolytic inhibitors (2-DG and 3-Br) were evaluated by MTT, colony formation and transwell assays. The results revealed that glycolytic inhibitor treatment decreased the proliferation, colonization, and migration ability of PAAD cells compared with those of CPT1A-overexpressing cells (Figures 5D–5G, S4B, and S4C). Moreover, treatment with the glycolytic inhibitors significantly attenuated the facilitation of EMT by CPT1A in PAAD cells (Figure 5H). The above results suggested that CPT1A could induce the malignant transformation of PAAD cells by activating the glycolytic pathway.

CPT1A regulates glycolytic activity and progression in pancreatic adenocarcinoma in a manner dependent on the stability of the Snail protein

As a key factor in the EMT process, the expression of the Snail protein was markedly increased and decreased in CPT1A-overexpressing and CPT1A-knockdown cells, respectively (Figure 4E), but no difference in its mRNA expression level was observed in sh-CPT1A cells (Figure 6A). Thus, we hypothesized that CPT1A might accelerate tumor development through Snail in PAAD. To test this hypothesis, Co-IP assay was performed and showed the potential binding interaction between CPT1A and Snail (Figure 6B). The results revealed that the Snail protein was markedly degraded in a time-dependent manner upon treatment with CHX in BxPC-3 vector cells, while there was no difference in Snail protein degradation in CPT1A-overexpressing cells (Figure 6C), revealing that CPT1A prolonged the half-life of the Snail protein. In addition, knockdown of CPT1A apparently enhanced the ubiquitylation of Snail (Figure 6D), proving that CPT1A regulates Snail protein stability through ubiquitylation.

More relevantly, a number of rescue assays were performed, including MTT, colony formation, and migration assays, and the results showed that knockdown of Snail suppressed the growth and migration of PAAD cells with CPT1A overexpression (Figures 6E–6G). Thus, the same directional trends were assessed by utilizing glucose levels and ATP assays (Figure 6H). Western blotting showed that knockdown of Snail reversed the downregulation of E-cadherin induced by CPT1A overexpression and blocked the expression of Vimentin and glycolytic

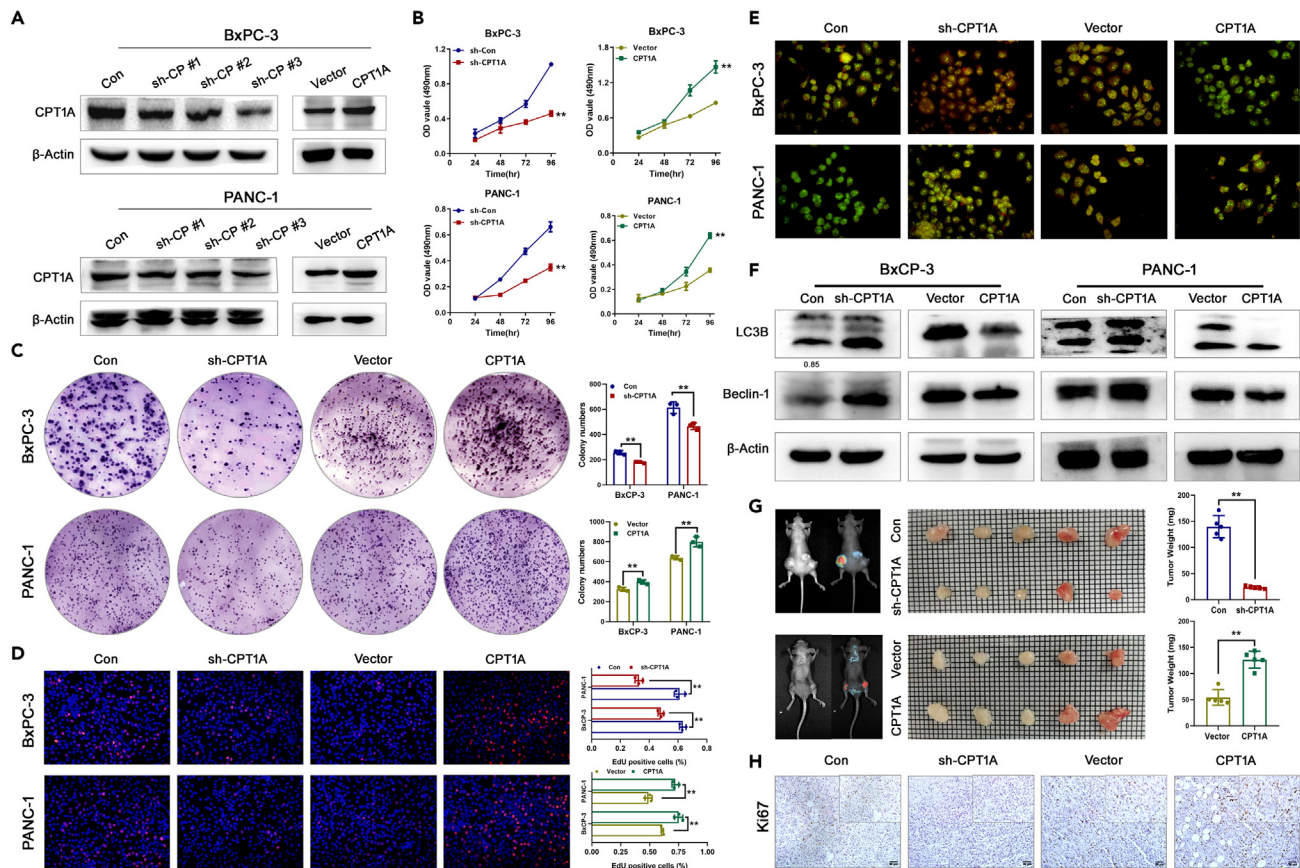


Figure 3. CPT1A enhances tumorigenesis *in vitro* and *in vivo*

(A) Western blot was performed to test the stable establishment effects of CPT1A knockdown and overexpression in PAAD cell lines.

(B–D) Cell proliferation ability was tested by MTT (B), colony formation (C) and EdU assays (D).

(E) The formation of autophagosomes was evaluated by AO staining. Magnification: 200 \times .

(F) Western blot was detected the expression of autophagic process markers (LC3-II and Beclin-1) in the constructed PAAD cells.

(G) The nude mice xenograft model evaluated the effect of CPT1A differential expression on tumor volume and weight. Size of each grid: 1 mm \times 1 mm.

(H) IHC staining showed Ki67 expression in tumor specimens from xenografts. Magnification: 200 \times . * $p < 0.05$ and ** $p < 0.01$.

markers induced by CPT1A overexpression (Figures 6I and S2F). Accordingly, CPT1A interacts with Snail, and CPT1A/Snail participate in glycolytic activity and progression in PAAD.

DISCUSSION

Recent studies have shown that there is a 1.5- to 2.0-fold increase in the risk of developing pancreatic cancer in patients with type 2 diabetes mellitus.^{21,22} The hyperglycemia, which has been shown to enhance proliferation, promotes epithelial-mesenchymal transition and cancer stem cells' properties, and metastatic potential in PAAD.^{23–27} Metastasis is another leading cause of death in patients with PAAD, and thus, identifying and suppressing metastasis-controlling genes and pathways can decrease the mortality rate of patients with PAAD. Recently, accumulated evidence has indicated the functions of CPT1A in cancer development include mediating metastasis and radiation resistance.²⁸ These prometastatic effects lead to overexpression of CPT1A in various tumors, such as breast cancer, and can regulate histone acetylation and VEGFR-3 signaling, thus increasing the malignancy degree of cancers.²⁹ Studies have shown that the ectopic activation of CPT1A participates in anoikis, chemosensitivity, tumorigenesis, and FAO in cancers and is associated with Rab14 expression, and succinylation of S100A10 in VEGF pathways.^{30–32} Here, we revealed that overexpression of CPT1A could indicate poor prognosis in patients with PAAD and was related to clinical stage, grade, LN metastasis and a shorter survival time in patients with PAAD. However, GEPIA database showed that high expression of CPT1A had a longer or shorter OS in different cancers (Figures 1G and 1H, all $p < 0.05$). It may be related to the tumor heterogeneity, and the expression levels and molecular mechanism of gene are different in different cancer. Taken altogether, abnormal expression level of CPT1A was closely related with the malignant progression and prognosis of patients with cancer. Moreover, we focused on the regulatory mechanisms of CPT1A in autophagy, EMT, and glycolysis in PAAD. However, the regulatory effects of CPT1A in BxPC-3 are better than in PANC-1. The difference may be related to the natural inhibitor malonylCoA in two cell lines.

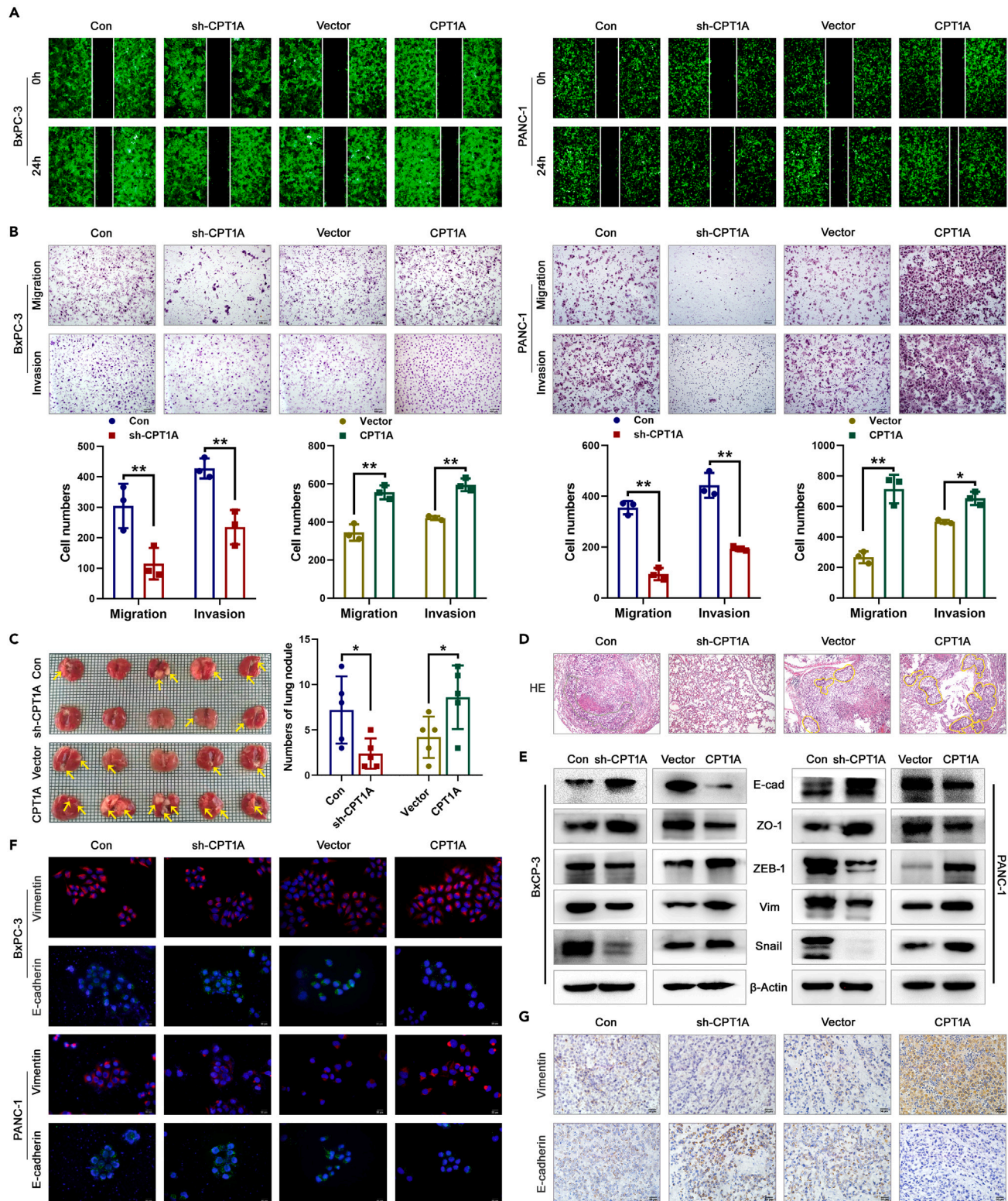


Figure 4. CPT1A induces the migration, invasion and promotes EMT process

(A) Wound healing demonstrated CPT1A affects the lateral migration of PAAD cells.

(B) Transwell assay showed CPT1A affects longitudinal migration and invasion abilities of PAAD cells.

Figure 4. Continued

(C and D) The four groups of BxCP-3 cells were injected into the nude mice respectively via tail vein for *in vivo* metastasis (n = 5 per group). Representative images showed the number of lung metastasis nodules (C), and HE staining (D) of the lung tissues. Size of each grid: 1 mm × 1 mm. Scale bar: 100 μm.

(E) Western blot assay was used to detect the effects of CPT1A differential expression on the protein expression level of EMT markers.

(F and G) IF (F) and IHC staining (G) were used to observe protein expression and localization of EMT markers in PAAD cells after CPT1A knockdown and overexpression. *p < 0.05 and **p < 0.01.

Unlike in most other solid tumors, robust extracellular matrix formation is induced in PAAD, resulting in two signature features of PAAD: glycolytic metabolism and a severely hypoxic environment.³³ As a result, PAAD cells utilize glycolytic metabolic reprogramming to meet their extravagant energy requirements and promote malignant behaviors, namely, growth and metastasis.^{34,35} Epidemiologic studies have emphasized that obesity and glucose levels are independent prognostic factors in patients with PAAD (Hu et al., 2021) and may be associated with the abnormal regulatory mechanism of CPT1A in gluconeogenesis and glucose homeostasis (Conti et al., 2011).^{36,37} Peng et al.¹⁹ proved that increased CPT1A expression in cancer-associated fibroblasts (CAFs) promotes anaerobic glycolysis, leading to CRC cell growth. The current study first established that CPT1A-regulated glycolysis leads to the progression and metastasis of PAAD. Moreover, autophagy as a key regulator of glucose homeostasis is mediated through autophagolysosome formation in cells with glycolytic metabolism and plays a dual role in cancer.³⁸ To date, most studies have shown that autophagy deficiency promotes PAAD but still functions as a tumor suppressor. Jiang et al.³⁹ demonstrated that knockdown of CPT1A could be a valid method to cure patients with osteoarthritis via the autophagy pathway. In addition, You et al.⁴⁰ found that PGRMC1 induces autophagy by increasing FAO, whereas CPT1A knockdown inhibits FAO but enhances FAS by increasing the expression of ACC, CD36, and LC3B. Mechanistically, PGRMC1 promotes autophagy by directly binding to a critical component of the autophagic machinery, LC3, resulting in increased LC3 cleavage and degradative autophagic activity. Consistent with the above data, our findings confirmed that CPT1A could regulate autophagy in PAAD cells by activating the glycolytic pathway. We hypothesized that this effect might be associated with the activation of autophagy to prevent glycolytic metabolism in PAAD cells when CPT1A expression was downregulated. In addition, a previous study showed for the first time that as a metabolic activator, CPT1A could induce FAO and drive the stemness of pancreatic precursor lesions,¹¹ and similar observations were confirmed in glioblastoma by Sperry et al.⁴¹ In addition, some data have proven that CPT1A integrates the metabolic flux from glycolysis to FAO in peritoneal metastatic CRC.¹⁹ However, the precise mechanism of CPT1A in the switch from glycolysis to FAO in PAAD cells needs further in-depth investigation.

It is widely known that PAAD cells possess plasticity, which leads to a bidirectional transition between epithelial and mesenchymal states.⁴² Zhao et al. exposed the mechanism of crosstalk between glycolysis and EMT phenotypes that promoted the migration of gemcitabine-resistant PAAD cells.⁴³ Glycolytic metabolism can also be involved in this crosstalk mechanism by supplying the energy needed for the EMT process in CRC cells,⁴⁴ and Wang et al.⁴⁵ proved that etomoxir, a CPT1 inhibitor, blocked fatty acid trafficking in GC cells, which was induced by CPT1A, thus preventing LN metastasis. Our study confirmed that the upregulation of CPT1A can lead to EMT, thereby facilitating metastasis. In addition, CPT1A-mediated glycolytic metabolism in PAAD cells can promote autophagy and metastasis. The above findings confirmed the interaction between lipid metabolism and EMT/autophagy, which may prove to be a breakthrough in the search for the mechanism of distant metastasis. Additionally, Zhao et al.⁴⁶ demonstrated that STIM1 shifted the metabolic pathway from aerobic glycolysis toward AMPK-activated FAO, which contributed to Snail-driven metastasis. CPT1A-mediated FAO also resulted in an increase in Snail expression to influence E-cadherin transcription in order to promote EMT in A549 cells, emphasizing the central role of Snail in the FAO-induced metastasis.⁴⁷ We hypothesized that this effect might be closely connected with the short and half-life and instability of the Snail protein and that Snail can bind to the promoter region of E-cadherin to suppress the expression of E-cadherin.⁴⁸ Mechanistically, this study revealed that CPT1A could regulate Snail stability by ubiquitylation and that the CPT1A/Snail axis could influence the growth, EMT, and, to a certain extent, glycolytic metabolism of PAAD cells.

Overall, our findings proved that CPT1A is overexpressed in PAAD tissues and that its overexpression is closely connected with the poor outcome of patients with PAAD. Moreover, we supplied a conceptual framework in which CPT1A/Snail accelerates autophagy and EMT by enhancing glycolytic metabolism in PAAD. These findings revealed that the CPT1A/Snail axis is closely linked with the progression of PAAD and might be a therapeutic target in PAAD.

Limitations of the study

Our data demonstrate that revealed Snail-dependent glycolysis as a crucial metabolic pathway by which CPT1A accelerates PAAD progression. Although our data suggested that CPT1A regulates glycolytic activity and progression in PAAD by regulating Snail stability. Further study is needed to elucidate the specific sites of CPT1A regulated Snail ubiquitination. Moreover, CPT1A is the key rate-limiting enzyme of FAO, which promotes PAAD progression and metastasis by activating the glycolytic pathway. However, the precise mechanism of CPT1A in the switch from glycolysis to FAO in PAAD cells needs further in-depth investigation.

STAR★METHODS

Detailed methods are provided in the online version of this paper and include the following:

- KEY RESOURCES TABLE
- RESOURCE AVAILABILITY

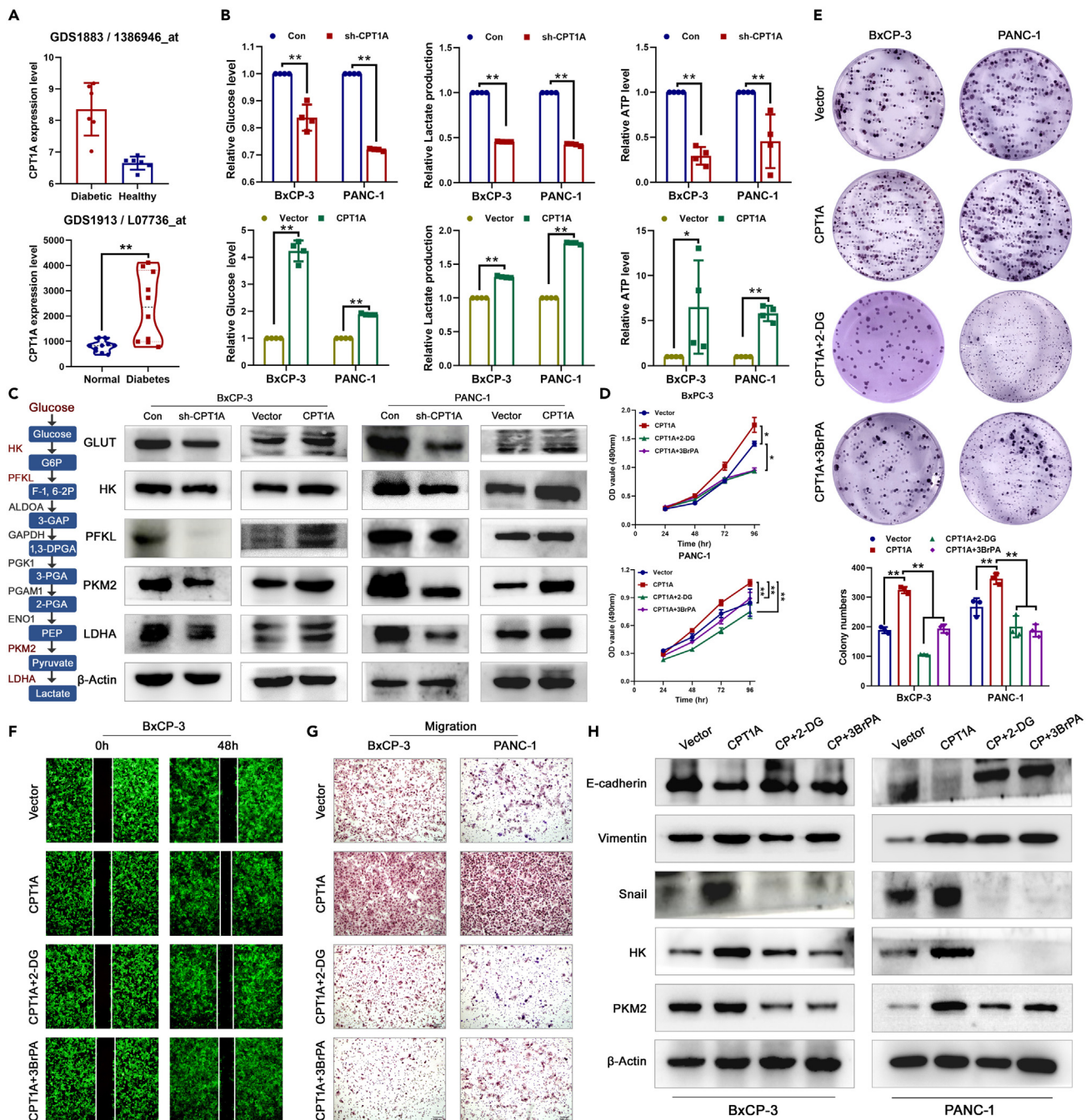


Figure 5. CPT1A promotes the progression of PAAD through glycolysis metabolism

(A) GEO database (GDS1881 and GDS1913) was analyzed the CPT1A expression level in different groups of rattus norvegicus.

(B) Metabolic kits were detected the glucose, ATP and lactate levels in PAAD cells.

(C) Western blot was analyzed the glycolysis markers (GLUT, HK2, PFKL, PKM and LDHA) expression levels.

(D–G) MTT (D), colony formation (E), wound healing (F) and migration (G) were used to test the proliferation and migration abilities of CPT1A overexpression cell after adding glycolysis inhibitors (2-DG and 3BrPA).

(H) Western blot was measured the expression levels of glycolysis and EMT markers. * $p < 0.05$ and ** $p < 0.01$.

- Lead contact
- Materials availability
- Data and code availability

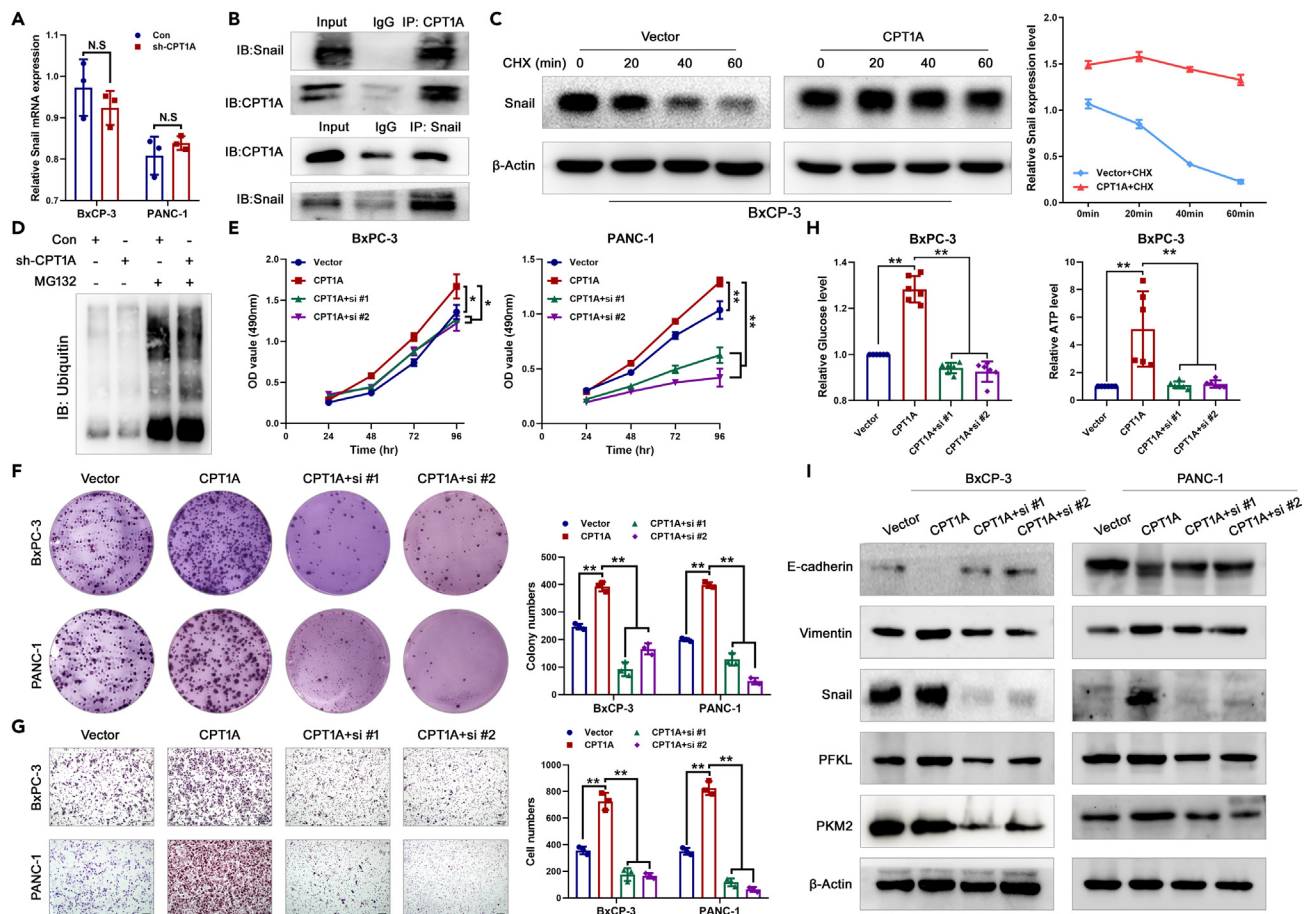


Figure 6. CPT1A/Snail axis promotes the development of PAAD

(A) qRT-PCR was analyzed the mRNA expression of Snail in PAAD cells.
 (B) CoIP was detected the interaction between CPT1A and Snail.
 (C) BxPC-3 cells of vector and CPT1A overexpression groups were treated with 10 μ M CHX for 0, 20, 40, and 60 min, then cells were collected and lysed respectively. The half-life of Snail protein was detected by Western blotting and quantified by Prism software.
 (D) BxPC-3 cells of control and sh-CPT1A groups were pretreated with 10 μ M MG132 for 4 h. The ubiquitination levels of Snail were measured by IP experiments.
 (E and F) MTT (E) and colony formation (F) assays were detected the proliferation ability of CPT1A overexpression cells after knockdown Snail.
 (G) Transwell assay was detected the longitudinal migration abilities of cells in PAAD cells.
 (H) Metabolic kits were detected the glucose and ATP levels in PAAD cells.
 (I) Western blot demonstrated the changes of EMT and glycolysis makers expression after Snail knockdown. * $p < 0.05$ and ** $p < 0.01$.

● **EXPERIMENTAL MODEL AND STUDY PARTICIPANT DETAILS**

- Ethics approval and consent to participate
- Clinical samples
- Cell lines
- Mice

● **METHOD DETAILS**

- Antibodies
- Transfection
- Stable cell line generation
- Wound healing assay
- Immunofluorescence (IF)
- Cell invasion and migration assays
- Methyl thiazolyl tetrazolium (MTT) and colony formation assays
- 5-ethynyl-2'-deoxyuridine (EdU) assay
- Western blot

- Immunohistochemistry (IHC)
- Immunoprecipitation (Co-IP) and detection of ubiquitination
- Glucose, lactate and ATP production testing
- Acridine orange (AO) staining
- *In vivo* tumorigenesis and metastasis assays
- Bioinformatics analysis
- **QUANTIFICATION AND STATISTICAL ANALYSIS**

SUPPLEMENTAL INFORMATION

Supplemental information can be found online at <https://doi.org/10.1016/j.isci.2023.107869>.

ACKNOWLEDGMENTS

We thank Professor Chunji Han [Key Laboratory of Pathobiology (Yanbian University), State Ethnic Affairs Commission] for providing the support on statistics.

Funding: This research was supported by the National Natural Science Foundation of China (No.82160552), the National Natural Science Foundation of Jilin Province (No.210101207, YDZJ202201ZYTS245, YDZJ202201ZYTS225).

AUTHOR CONTRIBUTIONS

Shipeng Yang, Jishu Quan and Yang Yang conceived this study and takes responsibility for the quality of the data. Anna Han, prepared all figures. Shipeng Yang, Ying Liu, and Chunxiao Tang participated in the tissue sample selection and experiments. Zhenhua Lin and Yang Yang acquired data and played an important role in interpreting the results. Shipeng Yang and Yang Yang performed the data analysis and wrote the article. All authors read and approved the final article.

DECLARATION OF INTERESTS

The authors declare that they have no competing interests.

INCLUSION AND DIVERSITY

We support inclusive, diverse, and equitable conduct of research.

Received: April 26, 2023

Revised: August 10, 2023

Accepted: September 6, 2023

Published: September 9, 2023

REFERENCES

1. Siegel, R.L., Miller, K.D., Fuchs, H.E., and Jemal, A. (2022). Cancer statistics, 2022. *CA A Cancer J. Clin.* 72, 7–33.
2. Cronin, K.A., Lake, A.J., Scott, S., Sherman, R.L., Noone, A.M., Howlader, N., Henley, S.J., Anderson, R.N., Firth, A.U., Ma, J., et al. (2018). Annual report to the nation on the status of cancer, part I: National cancer statistics. *Cancer* 124, 2785–2800.
3. Nelson, J.K., Thin, M.Z., Evan, T., Howell, S., Wu, M., Almeida, B., Legrave, N., Koenis, D.S., Koifman, G., Sugimoto, Y., et al. (2022). USP25 promotes pathological HIF-1-driven metabolic reprogramming and is a potential therapeutic target in pancreatic cancer. *Nat. Commun.* 13, 2070.
4. Roe, J.S., Hwang, C.I., Somerville, T.D.D., Milazzo, J.P., Lee, E.J., Da Silva, B., Maiorino, L., Tiriach, H., Young, C.M., Miyabayashi, K., et al. (2017). Enhancer reprogramming promotes pancreatic cancer metastasis. *Cell* 170, 875–888.e20.
5. Cai, K., Chen, S., Zhu, C., Li, L., Yu, C., He, Z., and Sun, C. (2022). FOXD1 facilitates pancreatic cancer cell proliferation, invasion, and metastasis by regulating GLUT1-mediated aerobic glycolysis. *Cell Death Dis.* 13, 765.
6. Qin, C., Yang, G., Yang, J., Ren, B., Wang, H., Chen, G., Zhao, F., You, L., Wang, W., and Zhao, Y. (2020). Metabolism of pancreatic cancer: paving the way to better anticancer strategies. *Mol. Cancer* 19, 50.
7. Liu, L., Xie, B., Fan, M., Candas-Green, D., Jiang, J.X., Wei, R., Wang, Y., Chen, H.W., Hu, Y., and Li, J.J. (2020). Low-level saturated fatty acid palmitate benefits liver cells by boosting mitochondrial metabolism via CDK1-SIRT3-CPT2 cascade. *Dev. Cell* 52, 196–209.e9.
8. LeBleu, V.S., O'Connell, J.T., Gonzalez Herrera, K.N., Wikman, H., Pantel, K., Haigis, M.C., de Carvalho, F.M., Damascena, A., Domingos Chinen, L.T., Rocha, R.M., et al. (2014). PGC-1 α mediates mitochondrial biogenesis and oxidative phosphorylation in cancer cells to promote metastasis. *Nat. Cell Biol.* 16, 992–1003.
9. Porporato, P.E., Payen, V.L., Baselet, B., and Sonveaux, P. (2016). Metabolic changes associated with tumor metastasis, part 2: Mitochondria, lipid and amino acid metabolism. *Cell. Mol. Life Sci.* 73, 1349–1363.
10. Gupta, K., Vuckovic, I., Zhang, S., Xiong, Y., Carlson, B.L., Jacobs, J., Olson, I., Petterson, X.M., Macura, S.I., Sarkaria, J., and Burns, T.C. (2020). Radiation induced metabolic alterations associate with tumor aggressiveness and poor outcome in glioblastoma. *Front. Oncol.* 10, 535.
11. Nimmakayala, R.K., Rauth, S., Chirravuri Venkata, R., Marimuthu, S., Nallasamy, P., Vengoji, R., Lele, S.M., Rachagani, S., Mallya, K., Malafa, M.P., et al. (2021). PGC1 α -Mediated Metabolic Reprogramming Drives the Stemness of Pancreatic Precursor Lesions. *Clin. Cancer Res.* 27, 5415–5429.
12. Guo, X., Wang, A., Wang, W., Wang, Y., Chen, H., Liu, X., Xia, T., Zhang, A., Chen, D., Qi, H., et al. (2021). HRD1 inhibits fatty acid oxidation and tumorigenesis by ubiquitinating CPT2 in triple-negative breast cancer. *Mol. Oncol.* 15, 642–656.
13. Wu, C., Dai, C., Li, X., Sun, M., Chu, H., Xuan, Q., Yin, Y., Fang, C., Yang, F., Jiang, Z., et al. (2022). AKR1C3-dependent lipid droplet formation confers hepatocellular carcinoma

- cell adaptability to targeted therapy. *Theranostics* 12, 7681–7698.
14. Jariwala, N., Mehta, G.A., Bhatt, V., Hussein, S., Parker, K.A., Yunus, N., Parker, J.S., Guo, J.Y., and Gatzka, M.L. (2021). CPT1A and fatty acid beta-oxidation are essential for tumor cell growth and survival in hormone receptor-positive breast cancer. *NAR Cancer* 3, zcab035.
 15. Jeon, S.M., Chandel, N.S., and Hay, N. (2012). AMPK regulates NADPH homeostasis to promote tumour cell survival during energy stress. *Nature* 485, 661–665.
 16. Huang, D., Chowdhury, S., Wang, H., Savage, S.R., Ivey, R.G., Kennedy, J.J., Whiteaker, J.R., Lin, C., Hou, X., Oberg, A.L., et al. (2021). Multiomic analysis identifies CPT1A as a potential therapeutic target in platinum-refractory, high-grade serous ovarian cancer. *Cell Rep. Med.* 2, 100471.
 17. Schlaepfer, I.R., and Joshi, M. (2020). CPT1A-mediated Fat Oxidation, Mechanisms, and Therapeutic Potential. *Endocrinology* 161, bqz046.
 18. Yang, H., Deng, Q., Ni, T., Liu, Y., Lu, L., Dai, H., Wang, H., and Yang, W. (2021). Targeted Inhibition of LPL/FABP4/CPT1 fatty acid metabolic axis can effectively prevent the progression of nonalcoholic steatohepatitis to liver cancer. *Int. J. Biol. Sci.* 17, 4207–4222.
 19. Peng, S., Chen, D., Cai, J., Yuan, Z., Huang, B., Li, Y., Wang, H., Luo, Q., Kuang, Y., Liang, W., et al. (2021). Enhancing cancer-associated fibroblast fatty acid catabolism within a metabolically challenging tumor microenvironment drives colon cancer peritoneal metastasis. *Mol. Oncol.* 15, 1391–1411.
 20. Tian, T., Lu, Y., Lin, J., Chen, M., Qiu, H., Zhu, W., Sun, H., Huang, J., Yang, H., and Deng, W. (2022). CPT1A promotes anoikis resistance in esophageal squamous cell carcinoma via redox homeostasis. *Redox Biol.* 58, 102544.
 21. Li, D. (2012). Diabetes and pancreatic cancer. *Mol. Carcinog.* 51, 64–74.
 22. Andersen, D.K., Korc, M., Petersen, G.M., Eibl, G., Li, D., Rickels, M.R., Chari, S.T., and Abbruzzese, J.L. (2017). Diabetes, Pancreatogenic Diabetes, and Pancreatic Cancer. *Diabetes* 66, 1103–1110.
 23. Ito, M., Makino, N., Matsuda, A., Ikeda, Y., Kakizaki, Y., Saito, Y., Ueno, Y., and Kawata, S. (2017). High Glucose Accelerates Cell Proliferation and Increases the Secretion and mRNA Expression of Osteopontin in Human Pancreatic Duct Epithelial Cells. *Int. J. Mol. Sci.* 18, 807.
 24. Han, L., Ma, Q., Li, J., Liu, H., Li, W., Ma, G., Xu, Q., Zhou, S., and Wu, E. (2011). High glucose promotes pancreatic cancer cell proliferation via the induction of EGF expression and transactivation of EGFR. *PLoS One* 6, e27074.
 25. Rahn, S., Zimmermann, V., Viol, F., Knaack, H., Stemmer, K., Peters, L., Lenk, L., Ungefroren, H., Saur, D., Schäfer, H., et al. (2018). Diabetes as risk factor for pancreatic cancer: Hyperglycemia promotes epithelial-mesenchymal-transition and stem cell properties in pancreatic ductal epithelial cells. *Cancer Lett.* 415, 129–150.
 26. Jian, Z., Cheng, T., Zhang, Z., Raulefs, S., Shi, K., Steiger, K., Maeritz, N., Kleigrew, K., Hofmann, T., Benitz, S., et al. (2018). Glycemic Variability Promotes Both Local Invasion and Metastatic Colonization by Pancreatic Ductal Adenocarcinoma. *Cell. Mol. Gastroenterol. Hepatol.* 6, 429–449.
 27. Stolzenberg-Solomon, R.Z., Graubard, B.I., Chari, S., Limburg, P., Taylor, P.R., Virtamo, J., and Albanes, D. (2005). Insulin, glucose, insulin resistance, and pancreatic cancer in male smokers. *JAMA* 294, 2872–2878.
 28. Du, Q., Zhang, H., He, M., Zhao, X., He, J., Cui, B., Yang, X., Tong, D., and Huang, Y. (2019). PGC1 α /CEBPB/CPT1A axis promotes radiation resistance of nasopharyngeal carcinoma through activating fatty acid oxidation. *Cancer Sci.* 10, 2050–2062.
 29. Han, S., Wei, R., Zhang, X., Jiang, N., Fan, M., Huang, J.H., Xie, B., Zhang, L., Miao, W., Butler, A.C.P., et al. (2019). CPT1A/2-Mediated FAO Enhancement-A Metabolic Target in Radioresistant Breast Cancer. *Front. Oncol.* 9, 1201.
 30. Tan, Z., Xiao, L., Tang, M., Bai, F., Li, J., Li, L., Shi, F., Li, N., Li, Y., Du, Q., et al. (2018). Targeting CPT1A-mediated fatty acid oxidation sensitizes nasopharyngeal carcinoma to radiation therapy. *Theranostics* 8, 2329–2347.
 31. Wang, C., Zhang, C., Li, X., Shen, J., Xu, Y., Shi, H., Mu, X., Pan, J., Zhao, T., Li, M., et al. (2019). CPT1A-mediated succinylation of S100A10 increases human gastric cancer invasion. *J. Cell Mol. Med.* 23, 293–305.
 32. Xiong, Y., Liu, Z., Zhao, X., Ruan, S., Zhang, X., Wang, S., and Huang, T. (2018). CPT1A regulates breast cancer-associated lymphangiogenesis via VEGF signaling. *Biomed. Pharmacother.* 106, 1–7.
 33. Ashton, T.M., McKenna, W.G., Kunz-Schughart, L.A., and Higgins, G.S. (2018). Oxidative Phosphorylation as an Emerging Target in Cancer Therapy. *Clin. Cancer Res.* 24, 2482–2490.
 34. Xu, F., Huang, M., Chen, Q., Niu, Y., Hu, Y., Hu, P., Chen, D., He, C., Huang, K., Zeng, Z., et al. (2021). LncRNA HIF1A-AS1 Promotes Gemcitabine Resistance of Pancreatic Cancer by Enhancing Glycolysis through Modulating the AKT/YB1/HIF1 α Pathway. *Cancer Res.* 81, 5678–5691.
 35. Tan, P., Li, M., Liu, Z., Li, T., Zhao, L., and Fu, W. (2022). Glycolysis-Related LINC02432/Hsa-miR-98-5p/HK2 Axis Inhibits Ferroptosis and Predicts Immune Infiltration, Tumor Mutation Burden, and Drug Sensitivity in Pancreatic Adenocarcinoma. *Front. Pharmacol.* 13, 937413.
 36. Hu, J.X., Zhao, C.F., Chen, W.B., Liu, Q.C., Li, Q.W., Lin, Y.Y., and Gao, F. (2021). Pancreatic cancer: A review of epidemiology, trend, and risk factors. *World J. Gastroenterol.* 27, 4298–4321.
 37. Conti, R., Mannucci, E., Pessotto, P., Tassoni, E., Carminati, P., Giannessi, F., and Arduini, A. (2011). Selective reversible inhibition of liver carnitine palmitoyl-transferase 1 by teglicar reduces gluconeogenesis and improves glucose homeostasis. *Diabetes* 60, 644–651.
 38. Chu, Y., Chang, Y., Lu, W., Sheng, X., Wang, S., Xu, H., and Ma, J. (2020). Regulation of Autophagy by Glycolysis in Cancer. *Cancer Manag. Res.* 12, 13259–13271.
 39. Jiang, N., Xing, B., Peng, R., Shang, J., Wu, B., Xiao, P., Lin, S., Xu, X., and Lu, H. (2022). Inhibition of Cpt1a alleviates oxidative stress-induced chondrocyte senescence via regulating mitochondrial dysfunction and activating mitophagy. *Mech. Ageing Dev.* 205, 111688.
 40. You, J.H., Lee, J., and Roh, J.L. (2021). PGRMC1-dependent lipophagy promotes ferroptosis in paclitaxel-tolerant resistant cancer cells. *J. Exp. Clin. Cancer Res.* 40, 350.
 41. Sperry, J., Condro, M.C., Guo, L., Braas, D., Vanderveer-Harris, N., Kim, K.K.O., Pope, W.B., Divakaruni, A.S., Lai, A., Christofk, H., et al. (2020). Glioblastoma Utilizes Fatty Acids and Ketone Bodies for Growth Allowing Progression during Ketogenic Diet Therapy. *iScience* 23, 101453.
 42. Rodriguez-Aznar, E., Wiesmüller, L., Sainz, B., Jr., and Hermann, P.C. (2019). EMT and Stemness-Key Players in Pancreatic Cancer Stem Cells. *Cancers* 11, 1136.
 43. Zhao, H., Duan, Q., Zhang, Z., Li, H., Wu, H., Shen, Q., Wang, C., and Yin, T. (2017). Up-regulation of glycolysis promotes the stemness and EMT phenotypes in gemcitabine-resistant pancreatic cancer cells. *J. Cell Mol. Med.* 21, 2055–2067.
 44. Xia, S., Wang, X., Wu, Y., Zhou, T., Tian, H., Liu, Z., Li, L., Yan, Z., and Zhang, G. (2022). miR-22 Suppresses EMT by Mediating Metabolic Reprogramming in Colorectal Cancer through Targeting MYC-Associated Factor X. *Dis. Markers* 2022, 7843565.
 45. Wang, M., Yu, W., Cao, X., Gu, H., Huang, J., Wu, C., Wang, L., Sha, X., Shen, B., Wang, T., et al. (2022). Exosomal CD44 Transmits Lymph Node Metastatic Capacity Between Gastric Cancer Cells via YAP-CPT1A-Mediated FAO Reprogramming. *Front. Oncol.* 12, 860175.
 46. Zhao, H., Yan, G., Zheng, L., Zhou, Y., Sheng, H., Wu, L., Zhang, Q., Lei, J., Zhang, J., Xin, R., et al. (2020). STIM1 is a metabolic checkpoint regulating the invasion and metastasis of hepatocellular carcinoma. *Theranostics* 10, 6483–6499.
 47. Lyu, J., Pirooznia, M., Li, Y., and Xiong, J. (2022). The short-chain fatty acid acetate modulates epithelial-to-mesenchymal transition. *Mol. Biol. Cell* 33, br13.
 48. Liu, J., Wu, Z., Han, D., Wei, C., Liang, Y., Jiang, T., Chen, L., Sha, M., Cao, Y., Huang, F., et al. (2020). Mesencephalic Astrocyte-Derived Neurotrophic Factor Inhibits Liver Cancer Through Small Ubiquitin-Related Modifier (SUMO)ylation-Related Suppression of NF- κ B/Snail Signaling Pathway and Epithelial-Mesenchymal Transition. *Hepatology* 71, 1262–1278.

STAR★METHODS

KEY RESOURCES TABLE

REAGENT or RESOURCE	SOURCE	IDENTIFIER
Antibodies		
E-cadherin	Abcam	ab40772
Vimentin	Abcam	ab92547
ZO-1	Cell Signaling Technology	Cat# 13663
LDHA	Cell Signaling Technology	Cat# 43723
CPT1A	Cell Signaling Technology	Cat# 97361
PKM2	Cell Signaling Technology	Cat# 4053
HK	Cell Signaling Technology	Cat# 2024
GLUT	Cell Signaling Technology	Cat# 12939
LC3B	Cell Signaling Technology	Cat# 3868
Beclin 1	Cell Signaling Technology	Cat# 4122
β-Actin	Cell Signaling Technology	Cat# 4970
Ki67	Proteintech	No. 27309
ZEB-1	Proteintech	No. 21544
IgG	Santa Cruz Biotechnology	Cat. no. sc-2025
Snail	Proteintech	No. 13099
Bacterial and virus strains		
Lenti-shCPT1A-GFP	Cyagen Biosciences	N/A
Lenti-CPT1A-GFP	Cyagen Biosciences	N/A
Lenti-Vector	Cyagen Biosciences	N/A
Lenti-shSCR	Cyagen Biosciences	N/A
Biological samples		
PAAD tissue microarrays	Shanghai Outdo Biotech	N/A
Chemicals, peptides, and recombinant proteins		
Lipofectamine 3000	Invitrogen	L3000001
Fetal bovine serum	Transgene	FS201-02
DMEM medium	Gibco	11965092
Triton X-100	Beyotime	ST795
Alexa Fluor® 488-conjugated secondary antibody	Invitrogen	Cat. no. A31627
RIPA buffer	CWBIO	Cat. no. CW2333S
goat anti-rabbit IgG (H&L)	Bioworld Technology	Cat. no. bs12478
goat anti-mouse IgG (H&L)	Bioworld Technology	Cat. no. bs12478
Protein A/G PLUS-Agarose	Santa Cruz Biotechnology	Cat. no. sc-2003
PMSF	Beijing Solarbio Science & Technology	Cat. no. P0100
MG132	Selleck Chemicals	S2619
ubiquitin	Santa Cruz Biotechnology	Cat. no. sc-8017
Glucose kit	Nanjing Jiancheng Biological Engineering Institute	A154-1-1
Lactate kit	Nanjing Jiancheng Biological Engineering Institute	A020-2-2
ATP kit	Nanjing Jiancheng Biological Engineering Institute	A095-1-1
BSA	Beijing Solarbio Science & Technology	CAS:9048-46-8

(Continued on next page)

Continued

REAGENT or RESOURCE	SOURCE	IDENTIFIER
<i>Critical commercial assays</i>		
Cell-Light™ EdU Apollo® 488 <i>In Vitro</i> Imaging Kit	Guangzhou RiboBio	C10310-3
BCA Protein Assay Kit	Beijing Solarbio Science & Technology	PC0020
IP/Co-IP kit	Abcam	Cat. no. ab206996
<i>Experimental models: Cell lines</i>		
BxPC-3	ATCC	CRL-1687
PANC-1	ATCC	CRL-1469
<i>Experimental models: Organisms/strains</i>		
BALB/c nude	Beijing Vital River Laboratory Animal Technology	Congenic strain
<i>Oligonucleotides</i>		
siRNA for Snail	Guangzhou RiboBio	N/A
<i>Software and algorithms</i>		
SPSS 20.0 software	IBM Corp.	N/A
GraphPad Prism 8.0 software	Dotmatics	v8.0.2.263
ImageJ software	ImageJ	v1.53e
R software	portable version	v3.5.2

RESOURCE AVAILABILITY**Lead contact**

Further information and requests for resources and reagents should be directed to and will be fulfilled by the lead contact, Yang Yang (yangyang@ybu.edu.cn).

Materials availability

This study did not generate new unique reagents. All the cell lines used in this manuscript will be made available upon request. A material transfer agreement will be required prior to sharing of materials.

Data and code availability

Data reported in this paper will be shared by the [lead contact](#) upon request. This paper does not report original code. Any additional information required to reanalyze the data reported in this paper is available from the [lead contact](#) upon request.

EXPERIMENTAL MODEL AND STUDY PARTICIPANT DETAILS**Ethics approval and consent to participate**

This research was approved by the Ethics committees of Yanbian University Medical College in China and was conducted in compliance with the tenets of the Declaration of Helsinki. All the animal procedures were performed under the ethical guidelines of the Laboratory Animal Center of Yanbian University. All the authors consented to participate in this study.

Clinical samples

In accordance with the Declaration of Helsinki, the patients organized of this study supplied informed consent, and the patients agreed with using their tumor tissue samples for investigation. PAAD tissue microarrays were purchased from Shanghai Outdo Biotech Co. Ltd. (China), including 100 cases of PAAD tissue and 80 cases of normal tissue adjacent to cancer. Ethics approval for the use of commercial PAAD tissues was waived from the Medical Ethics Committee of Yanbian University Medical College. The PAAD tissue samples were collected with the approval of the Medical Ethics Committee of Yanbian University Medical College. In accordance with the World Health Organization (WHO), the classification criteria of tumors were to evaluate the histological grade of tumor in this study.

Cell lines

Human PAAD cell lines, BxPC-3 and PANC-1, were from the laboratory of Yanbian University Cancer Research Center. All cell lines were cultured in Dulbecco's modified eagle medium (DMEM) containing 10% fetal bovine serum (FBS) and penicillin-streptomycin (100U/mL) at

the standard environment of 37°C and 5% CO₂. All cell lines were acquired from the American Type Culture Collection (ATCC) in 2020, which the cells were authenticated by short tandem repeat (STR). The last time of all cell lines was tested at December 2021.

Mice

Forty of BALB/c nude (Congenic strain) male mice aged 4-5 weeks (18-20g) were maintained under specific pathogen-free (SPF) conditions (temperature, 21 ± 8°C; humidity, 40-60%; 12-h light/dark cycle; free access to standard sterile food and water) at the animal house at Yanbian University, Yanji, China. All animal procedures were approved by institutional animal ethics committee abiding by the ethical guidelines of the Laboratory Animal Center of Yanbian University.

METHOD DETAILS

Antibodies

Antibodies against E-cadherin (ab40772, 1:1000), Vimentin (ab92547, 1:1000) were purchased from Abcam (Boston, USA). ZO-1 (#13663, 1:1000), LDHA (#43723, 1:1000), CPT1A (#97361, 1:1000), PKM2 (#4053, 1:1000), HK (#2024, 1:1000), GLUT (#12939, 1:1000), LC3B (#3868, 1:1000), Beclin 1 (#4122, 1:1000) and β-Actin (#4970, 1:1000) were purchased from Cell Signaling Technology (Boston, USA). Antibodies against Ki67 (No. 27309, 1:1000), ZEB-1 (No. 21544, 1:1000), Snail (No. 13099, 1:1000) were purchased from Proteintech (Humanzyme, China).

Transfection

The Snail siRNAs (si-control, si-RNA1, si-RNA2 and si-RNA3) and si-Con were purchased from Ribobio (Guangzhou, China). The sequences of the siRNAs are presented in [Table S1](#). The sequence of the si-Con was not disclosed, which is a commercial product. Its product number is siN0000001-1-5 and product name is siR NC #1(5nmol). According to the KD effect ([Figure S6](#)), si-RNA1 and si-RNA2 were used in this study. Lipofectamine 3000 (Invitrogen) was used to transfect 30nM si-RNA according to the manufacturer's instructions.

Stable cell line generation

The Lenti-shCPT1A-GFP, Lenti-CPT1A-GFP, Lenti-Vector and Lenti-shSCR were purchased from [cyagen.com](#) (Guangzhou, China). The sequences of the Lenti-shCPT1A-GFP and Lenti-shSCR are presented in [Table S2](#). Cells were counted (about 1 × 10⁵ cells/well) and inoculated in the 6-well plates. Transfection was performed when the cells were in a suitable condition (The cells are complete, homogeneous, transparent and with few particles, but without no vacuoles. The culture medium is clear and transparent, and without suspended cells and fragments) and the culture medium without antibiotics was changed. Then Human Lenti-shCPT1A-GFP, Lenti-CPT1A-Green fluorescent protein (GFP) and Lenti-shSCR were packaged in HEK-293FT cells. For stableinfection, the volume of the diluent was calculated according to the multiplicity of infection (MOI) value of the virus, and the diluent was placed into cell culture medium and cultured for 48h in a 37°C incubator. Suitable concentration of puromycin was added to screen stable cells. Transfection efficiency was confirmed by Western blot.

Wound healing assay

The cells were routinely digested and placed in a 6-well plate, and cell wounds were created by scratching cells using a micropipette tip when the degree of fusion reached 90%-100% after cell adhesion. The medium was discarded and washed with 1 × PBS for three times to remove the floating cells, followed by adding serum-free medium. Then spontaneous cell migration was monitored using a Nikon inverted microscope at 0h, and 24h. Wound closure distance was measured at three independent wounds in each group. The gap size (treated/untreated%) was calculated by measuring the width of the wound as follows: Occupancy of wound area (%)=(24 occupancy of wound area)/0 h occupancy of wound area × 100. Wound area was measured for three independent wounds in each group using ImageJ (v1.53e) software (National Institutes of Health).

Immunofluorescence (IF)

The cells were grown in glass-covered six-well plates with 90% fusion. The cells were washed with slides, fixed with 4% paraformaldehyde for 15min, permeated with 0.5% Triton X-100 (Beyotime, China) and blocked with 3% BSA for 2h. The cells were incubated with 3% BSA primary antibody at 4°C overnight, washed with PBS for three times, and then incubated for 2h with 3% BSA secondary antibody (Invitrogen) labeled with Alexa Fluor 488. Finally, the cells were analyzed by Leica SP5II confocal microscopy.

Cell invasion and migration assays

Cell invasion and migration assays were conducted in 24-well plants, two chamber plates with high-throughput screening multiwell inserts (BD Biosciences, San Jose, CA, USA), which included 8-μm (pore size) polycarbonate filters. For cell invasion, 5 × 10⁴ cells were mixed into the upper chamber, medium with fibronectin (20 μg/mL) was put in the lower chamber, and the cells were cultured at 37°C for hours. For cell migration, 3 × 10⁴ cells were mixed into the upper chamber, medium without any fibronectin was put in the lower chamber, and the cells were cultured at 37°C for hours. Then, invaded or migrated cells were laid on 100% methanol for 30 min and dyed gentian violet solution for 10 min. Cells were counted under a microscope at ×200 magnification. Each assay was performed in duplicate and repeated three times.

Methyl thiazolyl tetrazolium (MTT) and colony formation assays

The cells of each group were vaccinated at a concentration of 10^4 cells per well in 96-well plates. After cell adherence, MTT solution (1mg/mL) was added and cultured for 4h with 100uL per well. MTT solution was abandoned, 100uL dimethyl sulfoxide was added to each well, and incubated for 10min with low-speed shock at room temperature, away from light. Then the optical density was measured at 550nm using an ELISA plate reader.

5-ethynyl-2'-deoxyuridine (EdU) assay

5-ethynyl- 2'-deoxyuridine (EdU) is a thymine nucleoside analogue. EdU, instead of thymidine, can be plugged into the replicating DNA molecule in cell proliferation, marking the newly synthesized DNA with Apollo fluorescent dye containing EdU. According to the reagent instructions, we made use Cell-Light™ EdU Apollo@488 *In Vitro* Imaging Kit (C10310-3, RiboBio, China) and analyzed by Leica SP5II confocal microscope.

Western blot

Western blot analysis was performed with standard methods. Briefly, Cell lysis and protein extraction. Equal amounts of proteins were separated by sodium dodecyl sulfate/polyacrylamide gel electrophoresis (SDS/PAGE) and blotted onto a polyvinylidene fluoride (PVDF) membrane from Millipore company. After sealing off 5% non-fat milk, the membrane was hatched overnight at 4°C with the primary antibody and then with horseradish peroxidase-coupled secondary antibody (Millipore). Signal was detected with enhanced chemiluminescence (Millipore).

Immunohistochemistry (IHC)

Tissue sections (PAAD tissue microarray and xenografts tissue section) were placed at room temperature, rewarmed, and conventionally dewatered in an oven at 65°C for 1h. 1% citric acid buffer was heated to boiling, and the sections were placed in buffer for antigenic thermal repair. 3% H₂O₂ was added to the tissue to block endogenous peroxidase. The primary antibody was diluted with antibody diluent and incubated overnight in a 4°C refrigerator. Reaction enhancement reagent, secondary antibody reagent and 3,3'-diaminobenzidine (DAB) color solution were dropped to observe the staining degree under the microscope, and PBS buffer was placed to terminate color development. Stain with hematoxylin and reverse blue with PBS buffer. The sheet was sealed with neutral resin, the drawing was taken under microscope, and statistical staining results. And All tissue specimens were examined and scored by two pathologists (Lin Z & Piao J) using a double-blind control method. Immunohistochemical analysis was performed using semi-quantitative score combined with positive area percentage and staining intensity. CPT1A positive staining intensity score (negative =0, weak =1, medium =2, strong =3) times the percentage of stained cells ($\leq 25\%$ =1, 26-50%=2, 51-75%=3, >75%=4) Calculate the staining index (value 0-12) We defined CPT1A immunostaining values 0-3 as normal expression and 4 or above as overexpression.

Immunoprecipitation (Co-IP) and detection of ubiquitination

Pretreatment of protein A/G magnetic beads (Santa Cruz Biotechnology): Put the magnetic beads on the magnetic frame, add PBS, mix and clean gently, the supernatant was discarded, cleaned three times, sealed with 0.2% BSA, mixed at 4°C and sealed for 1h. Conventional cell lysis, protein extraction, placed on ice standby. After removing PBS, the magnetic beads were mixed with cell lysate and incubated at 4°C for 1h. The supernatant was placed in a new EP tube, and the target antibody and IgG were added correspondingly (as the control group). The supernatant was mixed at 4°C and incubated overnight. The next day, the closed magnetic beads were added into the EP tube and incubated at room temperature for 6h. Discard the supernatant and added 200uL to the EP tube, 4°C gently mixed, 3 times, 5min each time, added appropriate amount of eluent into EP tube, incubating at room temperature for 20min. Added 20uL 3×SDS buffer solution, 95°C metal bath for 5min, samples were obtained for loading, and detected by western blot. For ubiquitination experiment, cells were treated with or without MG132 (10uM) for 6h before harvested in IP lysis buffer, followed by above steps and analysis by Western blot for Ubiquitin (Santa Cruz Biotechnology).

Glucose, lactate and ATP production testing

Glucose (A154-1-1), lactate (A020-2-2) and ATP (A095-1-1) kits were purchased from Nanjing Jiancheng Biological Engineering Institute Co., LTD. Under the same treatment conditions, after all groups of cell samples were collected, cleaned and broken in sequence, glucose, lactate and ATP production were tested in accordance with the instructions of the kits.

Acridine orange (AO) staining

Cells were cultured on coverslips and stained with 1 uM AO for 15 min, which was purchased from Sigma company in USA (A9231) and cleaned with PBS at RT in the dark. The formation of acidic vesicular organelles (AVOs) was measured under a fluorescence microscope (AO, bright red fluorescence in acidic vesicles).

In vivo tumorigenesis and metastasis assays

To assess the effect of CPT1A on tumorigenicity *in vivo*, BxPC-3 cells (3×10^6 cells, with Con/sh-CPT1A or Vector/ CPT1A) were injected subcutaneously into both the left (Con or Vector) and right (sh-CPT1A or CPT1A) thighs root of nude mice to construct subcutaneous tumor-forming model of nude mice (10 mice in each group, two groups). To establish the lung metastasis model in another 20 mice, BxPC-3 cells (0.1 mL , 1×10^6 cells/mouse, 5 mice/group, with Con/sh-CPT1A or Vector/ CPT1A) were intravenously injected into the tail vein of nude mice by using a 28-gauge syringe. The tumor volume (mm^3) in each mouse was measured by a Vernier caliper every 3 days and calculated as follows: Tumor volume = length \times width \times height $\times \pi / 6$. Mice were euthanized following 21 days for the xenograft study and 8 weeks for the lung metastasis experiment. The following humane endpoints were established: Tumor diameter $>2.0 \text{ cm}$, weight loss $>20\%$ and poor overall condition. None of the mice reached the humane endpoints in this study. To reduce suffering, mice were anesthetized with 2% isoflurane. Mice were then rapidly euthanized by cervical dislocation. Verification of death included cardiac and respiratory arrest, lack of reflexion and changes in mucosal color. After subcutaneous tumors were dissected, tumors were weighed using a digital balance (Mettler), fixed with 4% formalin (Biosharp) and embedded with paraffin to prepare sections for histology. Further immunohistochemical staining was performed to detect the expression levels of Vimentin, E-cadherin and Ki67 in xenografts tissue section. No metastatic nodules were found in the abdominal and thoracic organs of the subcutaneous xenograft mice. After death verification, lungs of the lung metastasis model mice were completely dissected. The lungs were fixed with 4% formalin (Biosharp), embedded in paraffin, cut into sections and stained with hematoxylin-eosin (H&E) for histopathological evaluation. Metastatic lung nodules were counted using a microscope (IX51; Olympus Corporation). Outliers were recognized and removed. No blinding was done. All experiments were approved by the the Medical Ethics Committee of Yanbian University Medical College.

Bioinformatics analysis

The Human Protein Atlas (HPA, <https://www.proteinatlas.org/>), TIMER (<https://cistrome.shinyapps.io/timer/>), UCSC (<http://genome.ucsc.edu/>), and GEPIA (gepia.cancer-pku.cn) databases were used to explore CPT1A expression in pan-cancer. Sangerbox (<http://sangerbox.com/home.html>) drew the relationship between CPT1A expression and patients' clinical stage, and the receiver operating characteristic (ROC) curve, Sankey diagram in pan-cancer and PAAD. The Kaplan-Meier Plotter (<http://kmpLot.com/analysis/index.php?p=service>) database was searched the relationship between CPT1A expression and the survival of pan-cancer patients. The GEO database was used to detect the relationship between CPT1A expression and diabetes. The cBioportal database (<http://www.cbioportal.org/>) contained large-scale cancer genomics data and provided the mutation frequency and mutation type of CPT1A.

QUANTIFICATION AND STATISTICAL ANALYSIS

Statistical analysis was performed using the SPSS 20.0 software, GraphPad Prism 8.0 software, Image J software, and R software (version 3.5.2). Statistical differences between two groups were determined using an unpaired t-test, while those between multiple groups were determined using a one-way ANOVA followed by Bonferroni test post hoc test (group ≥ 3). Quantitation of the cell number, colony number, wound gap closure and WB band integrated density were performed with ImageJ software (v1.53e; NIH). Chi-square test was used to determine the relationship between NQO1 protein expression and clinicopathological parameters. Kaplan-Meier method was used to draw the survival curve, and Log-rank test was used for survival analysis. The Renyi test was performed to generate the *P*-values when survival curves crossed over. Cox proportional hazards models were applied to evaluate the hazard ratios (HR) in uni- and multivariate logistic regression analyses. The value of $P < 0.05$ was recognized statistically significant.